JOURNAL OF Applied Polymer SCIENCE

Preparation and Characterization of Polypyrrole/Modified Multiwalled Carbon Nanotube Nanocomposites Polymerized *In Situ* in the Presence of Barium Titanate

M. Moniruzzaman,[1] S. Sahoo,[1] D. Ghosh,[1] C. K. Das,[1] R. Singh[2]
[1]Materials Science Centre, Indian Institute of Technology, Kharagpur 721302, India
[2]Defence Research and Development Organization, New Delhi, India
Correspondence to: C. K. Das (E-mail: ckd@matsc.iitkgp.ernet.in)

ABSTRACT: Polypyrrole (PPy) composites were prepared with both unmodified and amine-modified multiwalled carbon nanotubes (MWCNTs) in the presence and absence of barium titanate ($BaTiO_3$) by *in situ* oxidative polymerization. A uniform coating of PPy on the MWCNTs and $BaTiO_3$ surfaces was confirmed by field emission scanning electron microscopy and high-resolution transmission electron microscopy images. The structure of the pure and amine-modified MWCNTs were identified by Fourier transform infrared spectroscopy. The incorporation of $BaTiO_3$ enhanced the thermal stability and capacitance properties of the composites. The maximum specific capacitance and energy density values found for the PPy/amine-modified MWCNT/$BaTiO_3$ composites were 155.5 F/g and 21.6 W h/kg, respectively, at a scan rate of 10 mV/s. The maximum power density was found to be 385.7 W/kg for the same composite at a scan rate of 200 mV/s. Furthermore, the impedance spectra of the composites showed moderate capacitive behavior.
 J. Appl. Polym. Sci. 000: 000–000, 2012

KEYWORDS: conducting polymers; dielectric properties; nanocomposites; polypyrroles

Received 7 September 2011; accepted 15 June 2012; published online
DOI: 10.1002/app.38202

INTRODUCTION

Growing anxiety about pollution and global warming has provoked a great deal of research on energy storage and conversations from alternative sources.[1] Supercapacitors are considered to be promising energy storage devices because of their long cycle life and low maintenance cost.[2] They are considered to be the intermediate system of dielectric capacitors and batteries. Mainly, carbon-based materials, conducting polymers, and metal oxides have been used for supercapacitor electrodes. After their discovery in 1991 (by Sumio Iijima), carbon nanotubes (CNTs) have become very useful materials for various energy applications because of their high conductivity,[3,4] high surface area,[5–7] and high chemical stability. The specific capacitance of CNTs is very low (80 F/g)[8] compared to those of conducting polymers such as polyaniline,[9–11] polypyrrole (PPy),[12] and polythiophene.[13] However, the stability of conducting polymers during the charge/discharge process is very poor. A combination of CNTs and conducting polymers can enhance both the specific capacitance and thermal stability during the charge/discharge cycles. Among the conducting polymers, PPy has been widely used as a part of supercapacitor electrode materials because of its good chemical and thermal stabilities, easy synthesis, high specific capacitance, and high electrical conductivity in the doped state. Recently, metal oxide/carbon nanomaterial/conducting polymer composites have been used as electrodes for the construction of electronic double-layer capacitors. These are known as *electrochemical double-layer capacitors*. Metal oxides present an attractive alternative as an electrode material because of their high specific capacitance at low resistance and high thermal stability. Many metal oxides and hydroxides, such as NiO, $Ni(OH)_2$, MnO_2, Co_2O_3, IrO_2, FeO, TiO_2, SnO_2, V_2O_5, and MoO, have been studied as supercapacitor electrode materials.[14] Although these types of hybrid inorganic–organic nanocomposite materials are very promising in the electronic industries, none of these composites are used in the commercial production of electronic double-layer capacitors, and they are still in laboratory-scale research.

In this study, we prepared CNT/PPy composites with and without barium titanate ($BaTiO_3$) by the *in situ* oxidative polymerization method with ammonium persulfate (APS) as an oxidant. The morphology of these nanocomposites was analyzed by field emission scanning electron microscopy (FESEM) and high-resolution transmission electron microscopy (HR-TEM). The electrochemical properties of these hybrid nanocomposites were

Table I. Compositions of the Composites

Sample	Composition
PPyC	PPy/MWCNT
PPyAC	PPy/amine-modified MWCNT
PPyCB	PPy/MWCNT/$BaTiO_3$
PPyACB	PPy/amine-modified MWCNT/$BaTiO_3$

evaluated by cyclic voltammetry (CV). Thermogravimetric analysis (TGA) was performed to measure the thermal stabilities of the hybrid nanocomposites.

EXPERIMENTAL

Materials

Multiwalled carbon nanotubes (MWCNTs) were obtained from Iljin Nano Technology (Seoul, Korea, 95% purity and 40–50 nm diameter). Dicyclohexylcarbodiimide (DCC) was supplied by Spectrochem Pvt., Ltd. (Mumbai, India). Ethylenediamine (EDA), APS, cetyltrimethyl ammonium bromide (CTAB), and $BaTiO_3$ (particle size <3 μm) were supplied by Loba Chemie Pvt., Ltd. (Mumbai, India). Aniline and tetrahydrofuran were obtained from E. Merck, Ltd. (India, Mumbai).

Synthesis

Modification of the MWCNTs. We prepared acid-modified MWCNTs by treating the MWCNTs with a mixed acid of H_2SO_4 and HNO_3, where the weight ratio of H_2SO_4 to HNO_3 was 3 : 1 and the weight ratio of MWCNTs to mixed acid was 1 : 400. The solution was stirred at 60°C for 24 h to obtain the acid-modified MWCNTs. Then, the obtained solution was washed with distilled water and centrifuged. The resulting black-colored solution was dried at 110°C. The acid-functionalized MWCNTs were then added to a mixture of EDA and DCC in tetrahydrofuran (EDA/DCC/MWCNTs weight ratio = 25 : 25 : 1) and stirred for 48 h to obtain the amine-functionalized MWCNTs.[15]

Composite Preparation. In 600 mL of deionized water, 1.24 g of CTAB and 60 mg of MWCNTs were added at room temperature and sonicated for 1 h to obtain a well-dispersed suspension. Here, CTAB was used as surfactant to disperse the MWCNTs in water. Then, 0.6 mL of pyrrole was added to the solution followed by a further 10 min of sonication. After that, 100 mL of distilled water containing APS (2 g) was added to the previous mixture, and and the mixture was sonicated for further 10 min. The reaction mixture was kept in refrigerator at 1–5°C for 24 h. The resulting black precipitate was washed with distilled water and ethanol several times and filtered. The precipitate was dried at 100°C for 12 h. For the $BaTiO_3$-based composites, $BaTiO_3$ was added to the CTAB and MWCNTs (MWCNTs/$BaTiO_3$/PPy = 1 :4 : 10). The same procedure was followed to synthesize the amine-modified MWCNT/PPy composites. Pure PPy was synthesized by the same procedure without the addition of CNTs. The compositions of the composites are given in Table I.

Characterizations

Fourier Transform Infrared (FTIR) Spectroscopy. FTIR spectroscopy was performed with a NEXUS 870 FTIR (Thermo Nicolet Instrument Corp.) instrument (Eden Prairie, United States). The samples were prepared by the mixture of potassium bromide (KBr) and PPy composites at a weight ratio of 10 : 1, and the samples were pelletized.

FESEM. A Carl Zeiss-SUPRA 40 FESEM instrument (Peabody, USA) with an accelerating voltage of 5 kV was used to observe the morphology of the nanocomposites. Energy-dispersive X-ray (EDX) analyses of the composites were carried out by deposition of the samples on Al foil.

HR-TEM. The nanocomposites with both unmodified/modified MWCNTs and $BaTiO_3$ were analyzed by HR-TEM (JEOL, Japan 2100) to check the coating of the conducting polymer onto the CNTs.

X-ray Diffraction (XRD) Analysis. XRD analysis was carried out with a Regaku Ultima III instrument (Texas, USA) with an acceleration voltage of 40 kV and a current of 40 mA. Scanning was performed within a 2θ range of 20–70° at a scanning rate of 3°/min.

Electrochemical Characterization. The composites based on conducting PPy were investigated by a three-electrode probe method with CV (Gamry Instrument, 750 mA and 2 V, Grand Forks, USA).

TGA. TGA curves were recorded with a DuPont 2100 thermogravimetric analyzer (Warminster, USA). The TGA measurements were conducted at a heating rate of 10°C/min under an air atmosphere from 30 to 800°C.

RESULTS AND DISCUSSION

FTIR Study

The FTIR spectrum of the MWCNTs and acid-modified and amine-modified MWCNTs are shown in Figure 1. The characteristic peaks at 1710, 1276, 3432, and 2920 cm^{-1} in the acid-modified MWCNTs corresponded to the C═O stretching, C—O stretching, O—H stretching, and C—H stretching, respectively, of the COOH group. In the FTIR spectrum of the amine-modified MWCNT, the peak at 3258 cm^{-1} was designated as the absorption peak of —NH stretching. In the amine-modified

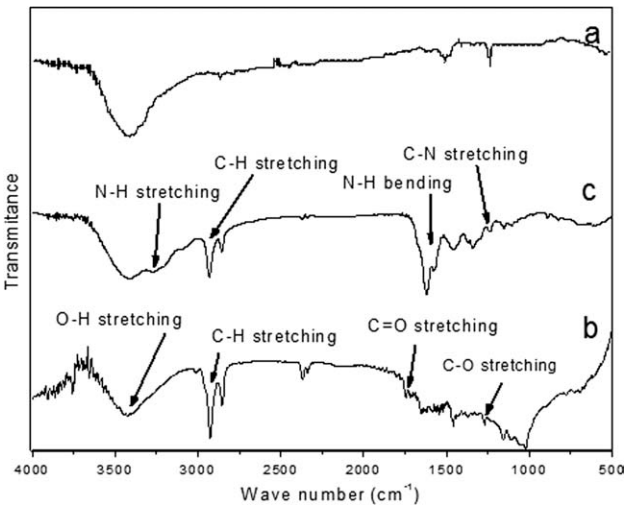

Figure 1. FTIR spectra of the (a) MWCNTs, (b) acid-modified MWCNTs, and (c) amine-modified MWCNTs.

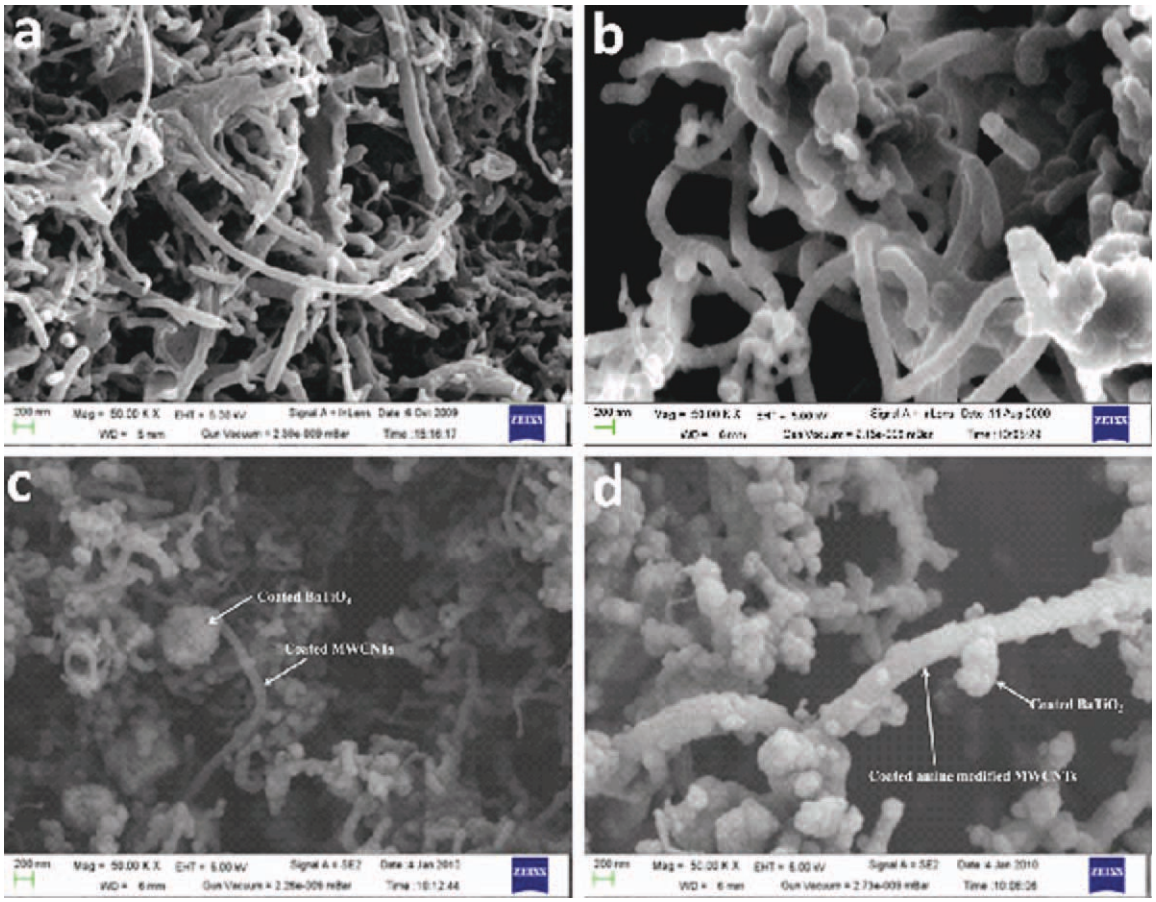

Figure 2. FESEM images of (a) PPyC, (b) PPyAC, (c) PPyCB, and (d) PPyACB. [Color figure can be viewed in the online issue, which is available at wileyonlinelibrary.com.]

MWCNTs, the characteristic peaks at 1238, 1576, and 2920 cm^{-1} were associated with C—N stretching, N—H bending, and C—H stretching, respectively. Thus, the FTIR spectra confirmed the acid and amine modification of the MWCNTs.

FESEM

The morphology of the composites was verified by FESEM. Figure 2(a–d) displays the FESEM images of the PPy composites, and it is clear that the PPy was uniformly coated onto the MWCNTs.[16,17] The average diameter of the PPy/MWCNTs composite was found to be 104 nm, whereas that of PPy/amine-modified MWCNTs was around 200 nm. This increase in the coating thickness was ascribed to the better affinity between the modified MWCNTs and pyrrole, which promoted the polymerization process on the surface of the modified MWCNTs. Similarly, the average diameters of the PPy/MWCNT/$BaTiO_3$ and PPy/amine-modified MWCNT/$BaTiO_3$ composites were 102 and 218 nm, respectively. The surfaces of the coated MWCNTs in the absence of $BaTiO_3$ were smooth in nature, whereas a rough morphology was evident for the composites prepared in the presence of $BaTiO_3$. A similar type of morphology was observed by Wang et al.[18] for the PPy/single-walled CNT composites. However, there were \many short CNTs coated by PPy, which were expected to be cut during the functionalization process. The qualitative EDX spectroscopy pattern of PPy/MWCNT/$BaTiO_3$ is shown in Figure 3 to confirm the presence of $BaTiO_3$. The EDX pattern of the composite clearly indicated the presence of Ba, Ti, and O. However, the signal of Al arose because of the Al foil, as the sample was deposited onto the foil when we performed the test.

HR-TEM

Figure 4 shows the HR-TEM images of the PPy composites in the presence and absence of $BaTiO_3$. The HR-TEM images

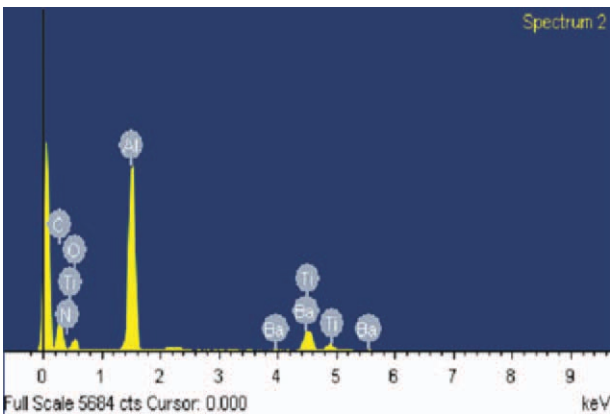

Figure 3. EDX of PPyCB (from FESEM analysis). [Color figure can be viewed in the online issue, which is available at wileyonlinelibrary.com.]

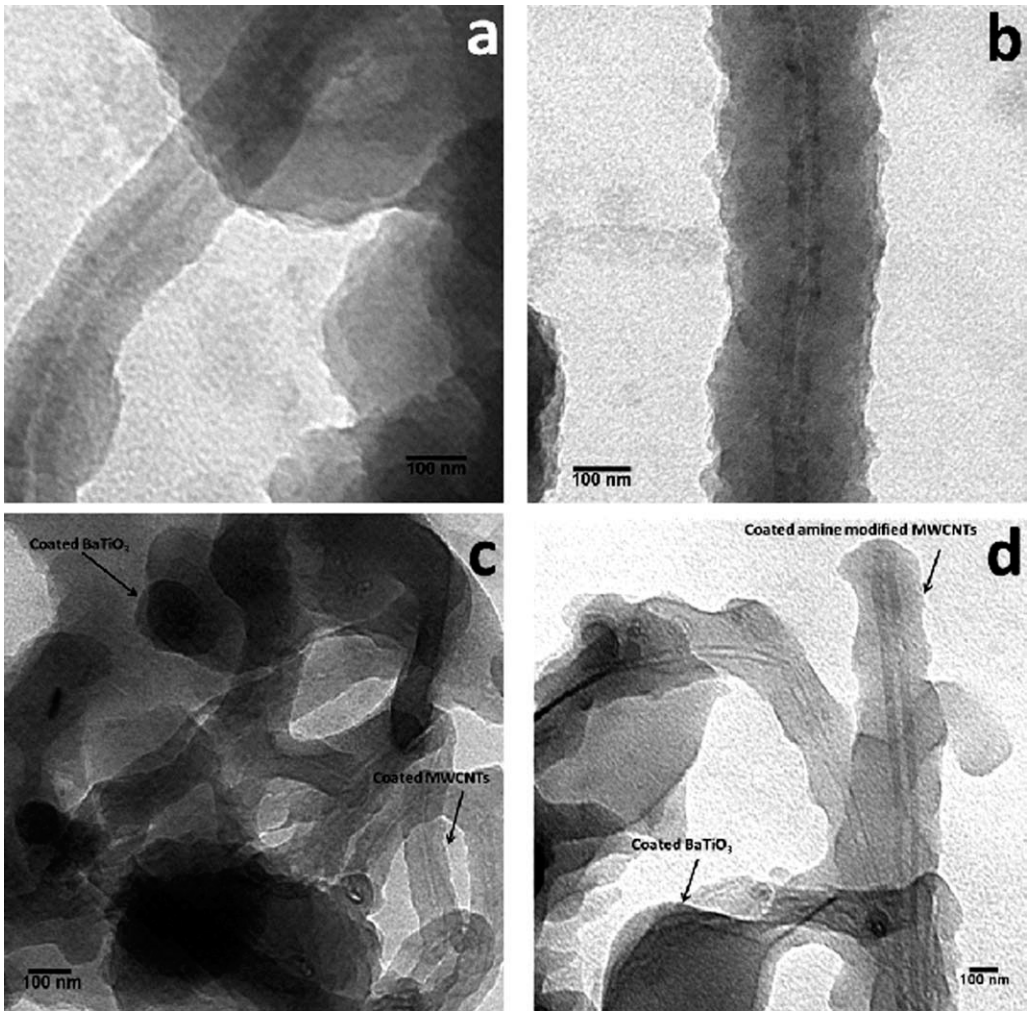

Figure 4. HR-TEM images of (a) PPyC, (b) PPyAC, (c) PPyCB, and (d) PPyACB.

confirmed that PPy was uniformly coated onto the MWCNT surface and the MWCNTs and $BaTiO_3$, respectively. The average outer diameter of the pure MWCNTs was around 40–50 nm, and the coating thickness of the concerned polymer was around 20 nm. For the amine-modified MWCNTs, the coating thickness of the polymer was around 40 nm. These results also supported the FESEM results. A similar kind of TEM morphology (CNT/PPy) was also observed by Xiao and Zhou.[19] The respective selected-area electron diffraction (SAED) images of the pure MWCNTs and PPyCB are given in Figure 5. The different diffraction spots (white dots) represented different crystal planes of the MWCNTs. However, such diffraction spots were absent in the SAED image of the composite because of the amorphous nature of the composite. Furthermore, EDX analysis were carried out in a TEM instrument by the deposition of the sample on a Cu grid through sonication, and the EDX curve of PPyCB is shown in Figure 6. All of the characteristic signals of $BaTiO_3$ were present, and the peak of Cu arose because of the Cu grid.

XRD Analysis

To confirm the presence of $BaTiO_3$ in PPyCB, XRD analysis was carried out, and the XRD pattern of PPyCB is shown in Figure 7. Peaks appeared at 2θ values of 22, 31.6, 39, 45.3, 51, 56.2, and 65.8° and were well indexed to the crystal planes at 100, 110, 111, 200, 210, 211, and 220 of $BaTiO_3$, respectively.[20] On the other hand, the characteristic peak appearing at 26° (2θ) corresponded to the crystal plane of the MWCNTs. Thus, XRD analysis of PPyCB confirmed the presence of $BaTiO_3$ in the composite.

Electrochemical Characterization

We prepared the electrode used for testing the electrochemical performances by pressing the material at a pressure of about 5 tons. For each composite, the electrode mass was 20 mg. All of the electrochemical experiments were carried out with a three-

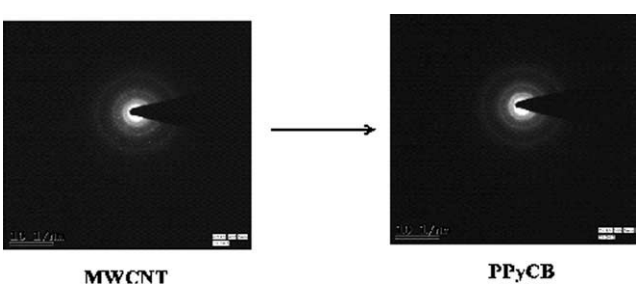

Figure 5. SAED images of the MWCNTs and PPyCB.

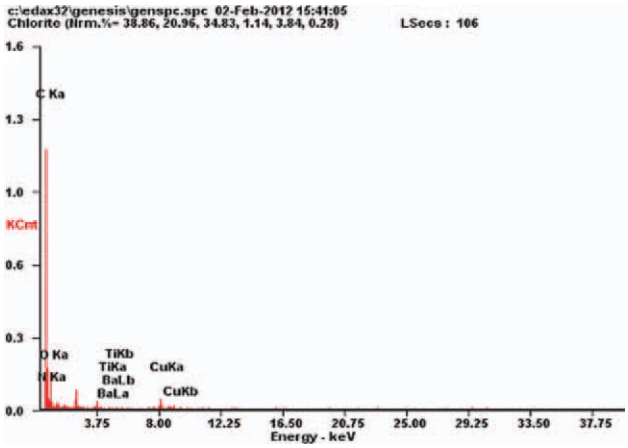

Figure 6. EDX of PPyCB (from HR-TEM analysis). [Color figure can be viewed in the online issue, which is available at wileyonlinelibrary.com.]

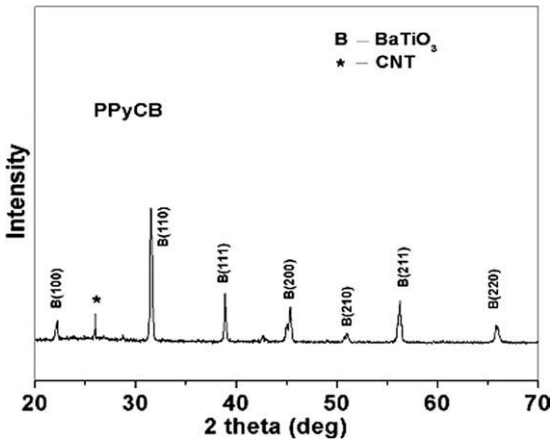

Figure 7. XRD curve of PPyCB.

electrode system in which platinum and a saturated calomel electrode were used as the counter and reference electrodes, respectively. A 1*M* KCl solution was used as the electrolyte for all of the electrochemical testing. CV measurements of the composite electrode were performed at different scan rates from 10 to 200 mV/s within the potential window of −0.4 to 0.6 V. The specific capacitance (C_{sp}) was calculated from the capacitive current (for nonrectangular shape) with the following formula[21,22]

$$C_{sp} = (I_+ - I_-)/vm$$

where I_+ and I_- were the maximum current in the positive voltage scan and the negative voltage scan, respectively; v is the scan rate; and m is the mass of the composite electrode material.

In case of the three-electrode cells, the capacitance values were considered to be the capacitance per electrode. Hence, taking into account that the proportion of CNTs in the composite was only 10 wt %, we determined the total capacitance to be mainly

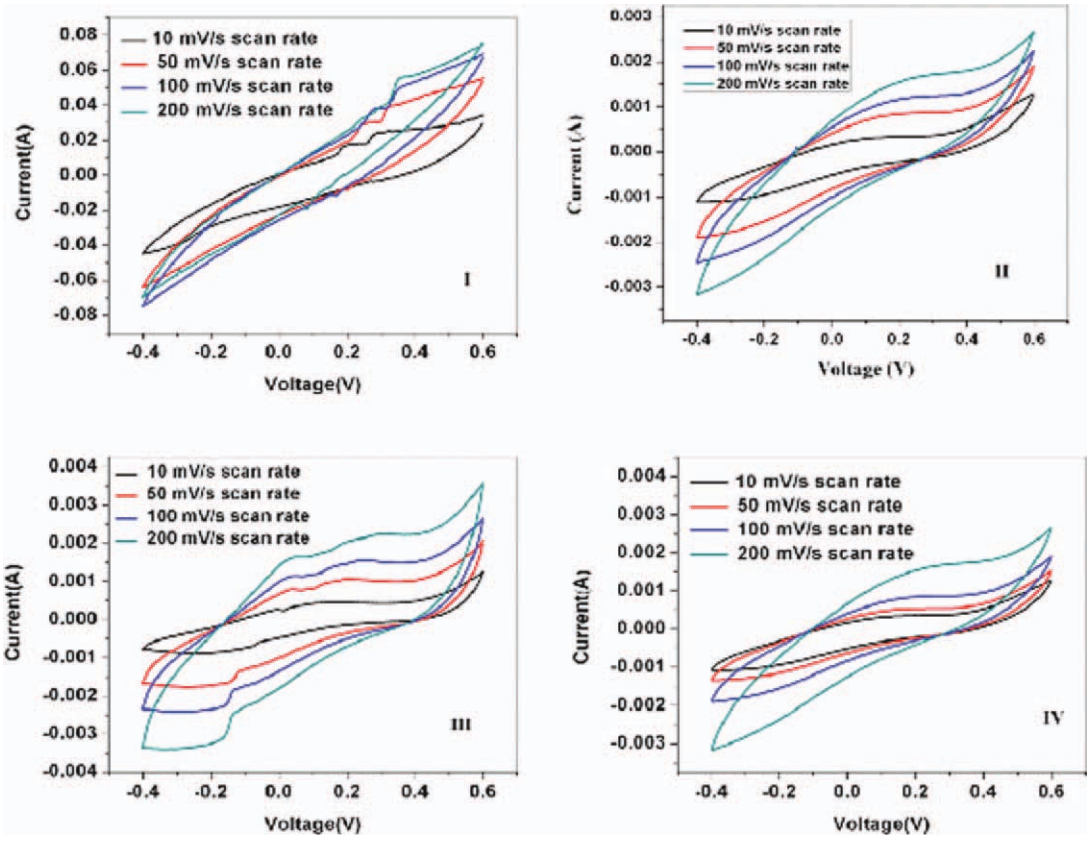

Figure 8. CV of the (I) pure PPy, (II) PPyC, (III) PPyAC, and (IV) PPyCB. [Color figure can be viewed in the online issue, which is available at wileyonlinelibrary.com.]

Table II. Specific Capacitance Values of the PPy Composites at Different Scan Rates

	Specific capacitance (F/g) at a scan rate of			
Sample	10 mV/s	50 mV/s	100 mV/s	200 mV/s
PPy	396.45	119.05	71.91	36.00
PPyC	128.5	38.04	23.6	14.7
PPyAC	106.7	38.7	25.5	17.6
PPyCB	116.1	28.6	18.7	14.4
PPyACB	155.5	62.2	39.2	25.1

due to the conducting polymer. On the other hand, $BaTiO_3$[23–25] was used to acquire a high thermal stability and to reduce the energy and power dissipation. The CNTs and $BaTiO_3$ assisted in the improvement of the thermal stability and reduced the swelling and shrinkage of the composite electrodes during multiple charging–discharging cycles.

Cyclic voltammograms of pure PPy and its composites are shown in Figure 8. The nonrectangular shape of the CV curves indicated redox behavior, which may have been due to the broad pore size distribution. The average capacitance value for the pure PPy was much large than that of the composites. The specific capacitance for PPy was found to be 396.45 F/g at a scan rate of 10 mV/s. However, for the composite materials, the specific capacitance was found to be very low. The decrease in capacitance may have been due to the fact that the electrolyte ions could not accumulate sufficiently at the conducting polymer–CNT/$BaTiO_3$ interface; this gave rise to the maximum specific capacitance values. The amine modification of CNT lowered the specific capacitance value of the composite. This may have been because of the fact that the modification of CNT increased the defects and decreased the electrical conductivity of the composite. Hence, the specific capacitance value decreased. The addition of $BaTiO_3$ to the PPy/MWCNT composites enhanced the capacitance properties because of the combined contribution of PPy and $BaTiO_3$ to the overall capacitance properties. Basically, for hybrid composites, including PPy/MWCNT, the overall capacitance value arose from the combination of the pseudocapacitance of PPy and the electrochemical double-layer capacitance of the MWCNTs. The incorporation of $BaTiO_3$ improved the pseudocapacitance properties, and hence, the overall capacitance value increased. However, among the composites, the highest specific capacitance was found to be 155.5 F/g for PPy/amine modified MWCNT/$BaTiO_3$. This value was higher than that of the RuO_2/MWCNT composite, as reported by Park et al.[26] Xiao and Zhou[19] successfully deposited PPy and poly(3-methylthiophene) on CNT and found a maximum capacitance of 87 F/g. Overall, for these composites, the conducting polymer (PPy) provided the pseudocapacitance, CNT acted as a minute electrode, and $BaTiO_3$ prevented the swelling and shrinkage of the electrode materials during the charging–discharging processes. These ternary effects of the components allowed the composite to show enhanced capacitance properties. With increasing scan rate, the specific capacitance values decreased because of the superior charge mobilization per unit time for all of the composites. The specific capacitance values of all of the composites at different scan rates are shown in Table II.

Energy Density. The energy density (E)[21,22,24] of the composites was calculated with the following equation:

$$E = {}^1\!/_2 CV^2$$

where C is the specific capacitance (F/g) and V is the operating voltage. The energy density of the composites showed the same trend as that of the capacitance. The maximum energy density in the PPy electrode among the PPy component was found to be 55.06 Wh/kg at a scan rate of 10 mV/s. However, among all of the composites, PPyACB showed the highest energy density of 21.6 Wh/kg at a 10 mV/s scan rate. The value obtained for PPyACB was higher than that of the conducting-polymer-based hybrid composite reported by Xiao and Zhou.[19] Detailed results of the energy density are shown in Table III.

Power Density. The power density (P)[21,22] of the composites was calculated by the following equation:

$$P = E/t$$

where t is the time for a complete cycle (s). The maximum power density was found in PPy (1798.69 W/kg) among the PPy components at scan rate of 200 mV/s. However, the highest power density of 385.7 W/kg was obtained for PPyACB at a 200 mV/s scan rate. The value obtained for PPyACB was higher than that of the asymmetric activated carbon/MnO_2/CNT composite (300 W/kg) reported by Xia and Huo.[27] With increasing scan rate, the power density of the composites decreased. Detailed results of the power density are shown in Table IV.

Impedance Study. Impedance measurement[25,28,29] was carried out for all of the composites in a 1M aqueous KCl solution (electrolyte) by potentiostatic electrochemical impedance

Table III. Energy Density of the PPy Composites at Different Scan Rates

	Energy density (Wh/kg) at a scan rate of			
Sample	10 mV/s	50 mV/s	100 mV/s	200 mV/s
PPy	55.06	16.53	9.99	5.00
PPyC	17.8	5.28	3.28	2.04
PPyAC	14.7	5.4	3.5	2.4
PPyCB	16.1	3.9	2.6	2.0
PPyACB	21.6	8.6	5.4	3.5

Table IV. Power Densities of the PPy Composites at Different Scan Rates

	Power density (W/kg) at a scan rate of			
Sample	10 mV/s	50 mV/s	100 mV/s	200 mV/s
PPy	983.26	1489.62	1796.19	1798.69
PPyC	320.4	475.2	590.4	734.4
PPyAC	262.9	484.2	635.7	876.7
PPyCB	287.7	353.5	465.9	719.4
PPyACB	385.7	775.8	978.0	1254.3

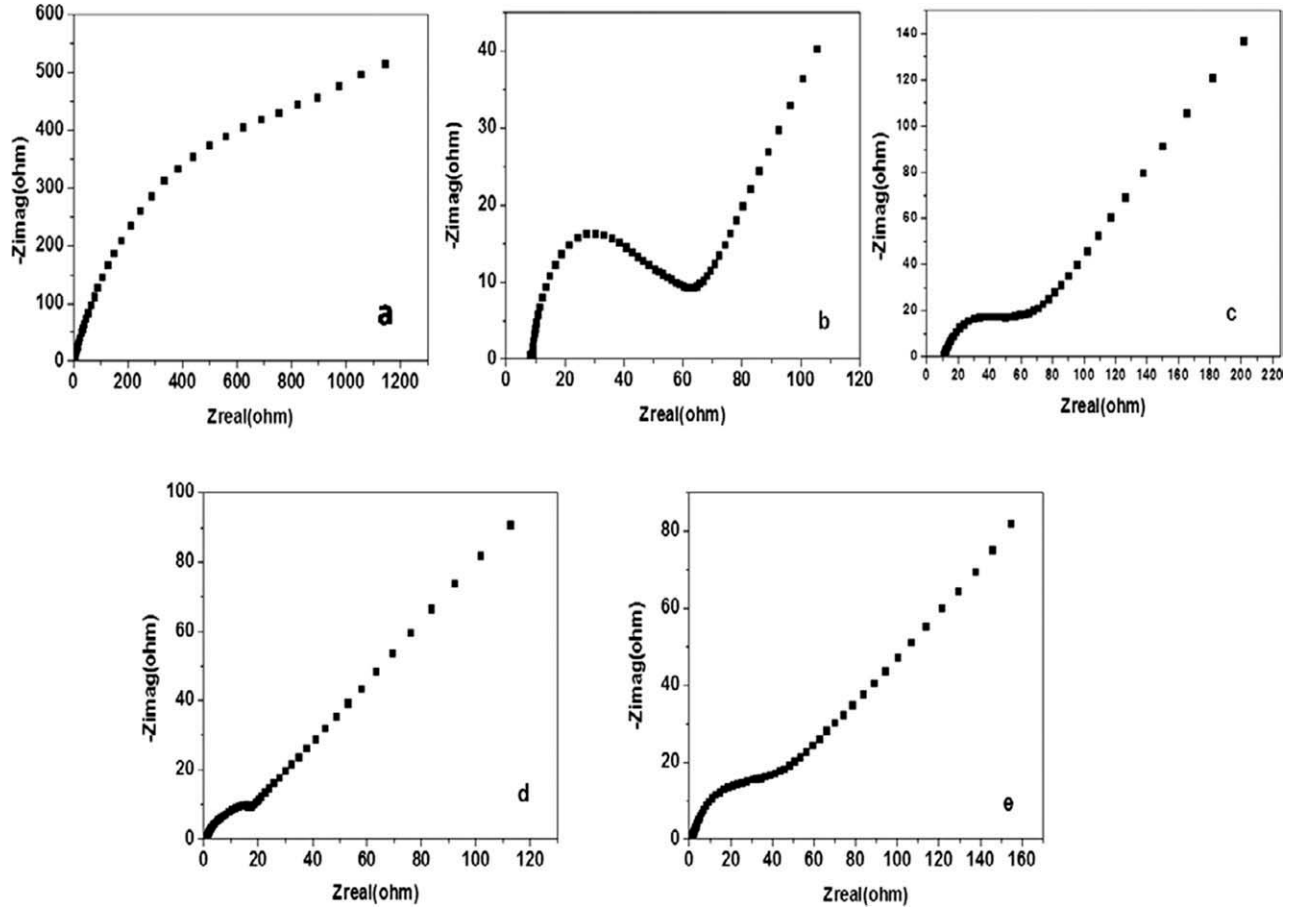

Figure 9. Impedance study of the (a) pure PPy, (b) PPyC, (c) PPyAC, (d) PPyCB, and (e) PPyACB. Zreal and Zimag represents the real and imaginary part of the impedence respectively.

spectroscopy. The electrochemical impedance spectroscopy curves of the PPy composites are shown in Figure 9. Two well-separated patterns were observed:

1. An arc was obtained at high frequencies; this was related to the interfacial processes.
2. A low-frequency region, which was an indication of a capacitive behavior related to the charging mechanism.

The difference in the real part of the impedance between low and high frequencies was used to evaluate the value of the electrochemical charge-transfer resistance (R_{ct}). In the case of PPy, the imaginary parts of the impedance at low frequencies were almost perpendicular to the real part at all potentials; this indicated a good capacitive behavior of the system at various discharging states. In the case of PPy/MWCNT, the R_{ct} value was 63 Ω. Again, the small values of R_{ct} in PPy/amine modified MWCNT could be explained by fast counter ions entering into or being ejected from the composite and the high conductance of the composite. The R_{ct} values decreased further in PPyCB and then increased again to 32 Ω in PPyACB. As a whole, the impedance spectra of the composites showed the moderate capacitor behavior of electrode materials.

Thermal Analysis

The thermal stabilities of the composites are depicted in Figure 10. We found that the thermal stabilities of the composites were much higher than that of the pure polymer. The amine modification of the CNTs enhanced the thermal stability of the composite; this may have been due to the better affinity[25] between the polymer and the amine-modified CNTs. However, the $BaTiO_3$-based composites showed a higher stability because of the improved stability of $BaTiO_3$ itself. However, from the TGA curves, it was clear that all of the composites were quite

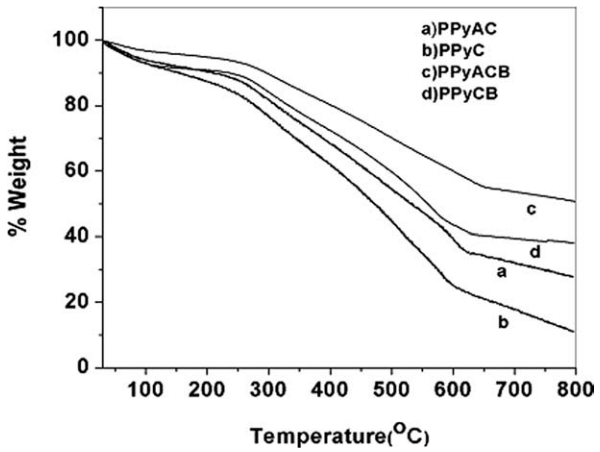

Figure 10. TGA curves of the PPy composites.

Table V. TGA Parameters of the PPy Composites

Sample	10% weight loss temperature (°C)	40% weight loss temperature (°C)
PPyC	153	410
PPyAC	208	460
PPyCB	235	497
PPyACB	293	598

stable up to 270°C. The first weight loss at 100°C mainly arose because of the intercalation of water molecules and some volatile components. For all of the composites, rapid degradation took place in the temperature range between 270 and 600°C. Table V demonstrates the detailed thermal studies of the composites.

CONCLUSIONS

Nanocomposites based on PPy and modified/unmodified MWCNTs in the presence and absence of $BaTiO_3$ were prepared by an *in situ* oxidative polymerization method. The advantages of the synthetic method were as follows:

1. It was simple.
2. There were no hazardous chemicals.
3. It gave a high product yield.
4. We produced supercapacitive electrode materials with enhanced electrochemical properties.

The incorporation of $BaTiO_3$ in composites improved the thermal stability, although the capacitance of $BaTiO_3$ containing hybrid composites was found to be lower compared to that of the pure polymer. However, the addition of this mixed metal oxide enhanced the capacitance properties of the composites. The as-prepared electrode materials had promising electrochemical properties for supercapacitor applications. However, further fabrication of the composites may show good application potential for supercapacitors or other power source systems.

REFERENCES

1. Arico, A. S.; Bruce, P.; Scrosati, B.; Tarascon. J.; Schalkwijk, W. V. *Nat. Mater.* **2005,** *4*, 366.
2. Kotz, R.; Carlen, M. *Electrochim Acta* **2000,** *45*, 2483.
3. Fisher, J. E.; Dai, R.; Thess, A.; Lee, R.; Hanjani, N. H.; Dehass, D. L.; Smalley, R. E. *Phys. Rev. B* **1997,** *55*, R4921.
4. De Heer, W. A.; Bacsa, W. S.; Chatelain, A.; Gerfin, T.; Baker, R. H.; Forro, L.; Ugarte, D. *Science* **1995,** *268*, 845.
5. Peigney, A.; Laurent, C.; Flahaut, E.; Bacsa, R. R.; Rousset, A. *Carbon* **2001,** *39*, 507.
6. An, K. H.; Kim, W. S.; Park, Y. S.; Choi, Y. C.; Lee. S. M.; Chung, D. C.; Bae, D. J.; Lim, S. C.; Lee, Y. H. *Adv. Mater.* **2001,** *13*, 497.
7. Shi, H. *Electrochim Acta* **1996,** *41*, 1633.
8. Niu, C.; Sichel, E. K.; Hoch, R.; Moy, D.; Tennent, H. *Appl. Phys. Lett.* **1997,** *70*, 1480.
9. Jang, J. *Adv. Polym. Sci.* **2006,** *199*, 189.
10. Gupta, V.; Miura, N. *Electrochem. Solid-State Lett.* **2005,** *8*, A630.
11. Ryu, K. S.; Kim, K. M.; Park, N. G.; Park, Y. J.; Chang, S. H. *J. Power Sources* **2002,** *103*, 305.
12. Jurewicz, K.; Delpeux, S.; Bertaggna, V.; Beguin, F.; Frackowiak, E. *Chem. Phys. Lett.* **2001,** *347*, 36.
13. Laforgue, A.; Simon, P.; Fauvarque, J. F.; Sarrau, J. F.; Lailler, P. *J. Electrochem. Sci.* **1999,** *80*, 142.
14. Jayalakshmi, M.; Balasubramanian, K. *J. Electrochem. Sci.* **2008,** *3*, 1196.
15. Yuen, S. M.; Ma, C. C. M.; Lin, Y. Y.; Kuan, H. C. *Compos. Sci. Tech.* **2007,** *67*, 2564.
16. Frackowaik, E.; Jurewicz, K.; Delpeux, S.; Beguin, F. *J. Power Sources* **2001,** *97–98*, 822.
17. Lota, K.; Khomenko, V.; Frackowiak, E. *J. Phys. Chem. Solids* **2004,** *65*, 295.
18. Wang, J.; Xu, Y.; Chen, X.; Sun, X.; *Compos. Sci. Tech.* **2007,** *67*, 2981.
19. Xiao, Q.; Zhou, X. *Electrochim Acta* **2003,** *48*, 575.
20. Yang, Y.; Wang, X.; Sun, C.; Li, L. *Nanotechnology* **2009,** *20*, 055709.
21. Sahoo, S.; Karthikeyan, G.; Nayak, G. C.; Das, C. K. *Synth. Met.* **2011,** *161*, 1713.
22. Moniruzzaman, M.; Das, C. K. *Macromol Symp* **2010,** *298*, 34.
23. Chandler, C. D.; Powell, Q.; Smith, M. J. H.; Kodas, T. T. *J. Mater. Chem.* **1993,** *3*, 775.
24. Conway, B. E. Electrochemical Supercapacitors; Kluwer Academic/Plenum: New York, **1999.**
25. Wang, Y.; Shi, Z.; Huang, Y.; Ma, Y.; Wang, C.; Chen, M.; Chen, Y. *J Phys Chem* **2009,** *113*, 13103.
26. Park, J. H.; Ko, J. M.; Parka, O. O. *J. Electrochem. Soc.* **2003,** *150*, A864.
27. Xia, H.; Huo, C. *Int. J. Smart Nano Mater.* **2011,** *2*, 283.
28. Qu, D. *J. Power Sources* **2002,** *109*, 403.
29. Yang, K.; Gu, M.; Jin, Y. *J. Appl. Polym. Sci.* **2008,** *110*, 2980.